



Investigations into dual-grating THz-driven accelerators



Y. Wei^{a,b,*}, R. Ischebeck^c, M. Dehler^c, E. Ferrari^c, N. Hiller^c, S. Jamison^d, G. Xia^{a,e},
K. Hanahoe^{a,e}, Y. Li^{a,e}, J.D.A. Smith^f, C.P. Welsch^{a,b}

^a Cockcroft Institute, Sci-Tech Daresbury, Warrington, WA4 4AD, United Kingdom

^b Physics Department, University of Liverpool, Liverpool, L69 3BX, United Kingdom

^c Paul Scherrer Institute (PSI), Villigen, 5232, Switzerland

^d Accelerator Science and Technology Centre, Sci-Tech Daresbury, Warrington, WA4 4AD, United Kingdom

^e School of Physics and Astronomy, University of Manchester, Manchester, M13 9PL, United Kingdom

^f Tech-X UK Ltd, Sci-Tech Daresbury, Warrington, WA4 4AD, United Kingdom

ARTICLE INFO

Keywords:

Dielectric dual-gratings
THz-driven
High gradient
Wakefield
THz-bunch interaction
Beam quality

ABSTRACT

Advanced acceleration technologies are receiving considerable interest in order to miniaturize future particle accelerators. One such technology is the dual-grating dielectric structures, which can support accelerating fields one to two orders of magnitude higher than the metal RF cavities in conventional accelerators. This opens up the possibility of enabling high accelerating gradients of up to several GV/m. This paper investigates numerically a quartz dual-grating structure which is driven by THz pulses to accelerate electrons. Geometry optimizations are carried out to achieve the trade-offs between accelerating gradient and vacuum channel gap. A realistic electron bunch available from the future Compact Linear Accelerator for Research and Applications (CLARA) is loaded into an optimized 100-period dual-grating structure for a detailed wakefield study. A THz pulse is then employed to interact with this CLARA bunch in the optimized structure. The computed beam quality is analyzed in terms of emittance, energy spread and loaded accelerating gradient. The simulations show that an accelerating gradient of 348 ± 12 MV/m with an emittance growth of 3.0% can be obtained.

© 2017 The Authors. Published by Elsevier B.V. This is an open access article under the CC BY license (<http://creativecommons.org/licenses/by/4.0/>).

1. Introduction

Dielectric structures have been found to withstand electric fields one to two orders of magnitude larger than metals at optical frequencies, thereby sustaining high accelerating gradients in the range of GV/m. These dielectric structures can be driven either by infrared optical or by THz pulses, enabling dielectric laser-driven accelerators (DLAs) and dielectric THz-driven accelerators (DTAs). Empirically, it is found that the RF-induced breakdown threshold E_s scales with frequency as $f^{1/2}$ and pulse duration as $\tau^{-1/4}$, as described in $E_s \propto f^{1/2} \tau^{-1/4}$ [1,2]. This indicates that in principle, DLAs can generate accelerating gradients higher than DTAs. DLAs have successfully demonstrated accelerating gradients of 300 MV/m [3] and 690 MV/m [4] for relativistic electron acceleration, and gradients of 25 MV/m [5], 220 MV/m [6] and 370 MV/m [7] for non-relativistic electron acceleration. However, DLAs suffer from low bunch charge and sub-femtosecond timing requirements due to the short wavelength of operation. In a DLA, a laser beam is used to accelerate particles through a microscopic channel in an artfully-crafted glass chip. Such a channel gap can be no wider than several

μm [3,4,8–12] in order to generate a high gradient of GV/m, which limits the transverse size and hence the bunch charge. Furthermore, for a laser wavelength of $2 \mu\text{m}$, the particle bunch has to occupy only a small fraction of the optical cycle in order to maintain good beam quality in terms of emittance and energy spread. If 1^0 of optical cycle is used, the total bunch length is only 5.6 nm, which also limits the particle bunch charge. In addition, the timing precision between the optical cycle and the arrival of the particle bunch is a practical concern. Using a laser wavelength of $2 \mu\text{m}$, a 1^0 phase jitter requires a timing jitter of < 20 as between the optical pulse and the particle bunch, which is challenging to maintain over long distances.

THz frequencies provide wavelengths two orders of magnitude longer than optical sources. In this situation, DTAs can be fabricated with conventional machining techniques due to the long wavelength of operation. This accommodates particle bunches with larger sizes and charges, which is more beneficial for bending and focusing [13] compared to DLAs. DTAs also provide a more accurate timing jitter than DLAs. For a THz wavelength of $600 \mu\text{m}$, 1^0 of optical cycle corresponds

* Correspondence to: The Cockcroft Institute, Daresbury Laboratory, Sci-Tech Daresbury, Warrington, WA4 4AD, United Kingdom.
E-mail address: yelong.wei@cockcroft.ac.uk (Y. Wei).

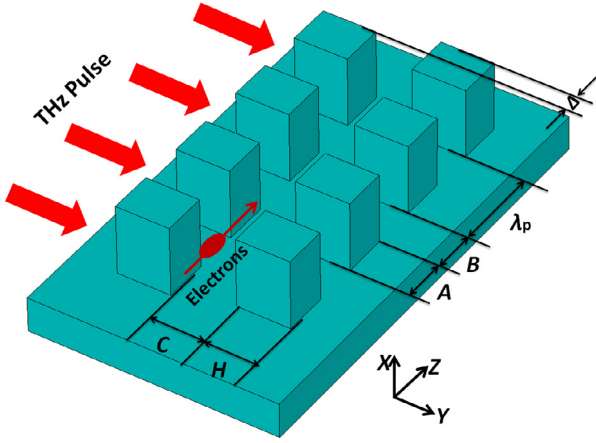


Fig. 1. Schematic of a dual-grating structure illuminated by a THz pulse. λ_p , A , B , C , H , and Δ represent grating period, pillar width, pillar trench, vacuum channel gap, pillar height and longitudinal shift, respectively; $A + B = \lambda_p$ is selected for all simulations.

to a $1.7 \mu\text{m}$ bunch length, while 1° of phase jitter requires a 5.6 fs timing jitter, which is readily achievable [14]. With recent advances in sources for the generation of THz, mJ pulse energy and extremely high electric fields in the GV/m have been achieved [15–17], which can boost the accelerating gradient up to GV/m for a DTA. Experiments have already demonstrated the acceleration of electrons in THz-driven dielectric structures [18–20]. Therefore, DTAs are holding great potential for reducing the size and cost of future particle accelerators.

In this paper a quartz dual-grating structure is investigated for accelerating electrons at THz frequencies. As shown schematically in Fig. 1, a short, intense THz pulse is used to illuminate a dual-grating structure, creating standing-wave-like electric field in the structure's channel gap where the electrons travel and are accelerated. In Section 2, geometry optimizations are performed in order to find the optimum dual-grating structure for the acceleration of relativistic electrons. It is then followed in Section 3 by a detailed wakefield study of an optimized 100-period dual-grating structure. Simulations are performed using the beam properties of the future Compact Linear Accelerator for Research and Applications (CLARA) [21] which is planned as an X-ray free electron laser (FEL) test facility located at the Daresbury laboratory in the UK. In Section 4, a linearly-polarized THz pulse is introduced to interact with the CLARA bunch in the optimized structure. The achievable beam quality is analyzed in terms of emittance, energy spread and loaded accelerating gradient. Finally the current challenges and limitations are discussed.

2. Geometry optimization

The dual-grating structure is a modification from the original design by Plettner et al. [8]. When a linearly-polarized THz pulse travels through the structure, the speed of the wave in vacuum is higher than that in the dielectric grating pillar. This produces the desired π phase difference in the vacuum channel for the wave front, resulting in periodic energy modulation for electrons traveling along the longitudinal z -axis.

In order to optimize such a dual-grating structure, VSim [22], based on a finite difference time domain (FDTD) method, is used to compute the electric and magnetic fields generated in the structure. The gratings are modeled as a 2-dimensional (y - z plane) structure to simplify our computations for the electric and magnetic fields. Periodic boundary conditions are applied along the electron channel in the z direction. Matched absorbing layers (MALs) are used along the laser propagation direction (y -axis) to absorb the transmitted wave. The mesh size is set to $\lambda_p/80$ so that the simulation results are converged to increase accuracy.

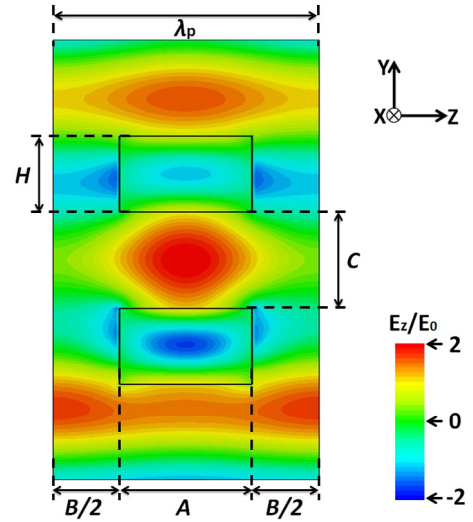


Fig. 2. Longitudinal electric field E_z distribution in a single unit dual-grating structure illuminated by a uniform plane wave with a field E_0 along y -axis.

A plane wave with a wavelength of $\lambda_0 = 150 \mu\text{m}$ and a field amplitude E_0 propagates in $+y$ and illuminates a single unit dual-grating structure, as illustrated in Fig. 2. A grating period of $\lambda_p = 150 \mu\text{m}$ is chosen so that the first spatial harmonic and relativistic electrons are synchronized [23]. The desired π phase difference for the wave front is achieved by setting pillar height $H = \frac{\lambda_0}{2(n-1)} = 0.50\lambda_0$, here quartz with a refractive index of $n = 2$ (Ref. [24]) is chosen due to its high damage threshold [18–20,25–27] and thermal conductivity.

The accelerating gradient G_0 is evaluated by $E_z[z(t), t]$ which is the longitudinal electric field integral along the vacuum channel center as shown in Fig. 2:

$$G_0 = \frac{1}{\lambda_p} \int_0^{\lambda_p} E_z[z(t), t] dz, \quad (1)$$

where λ_p is the grating period, $z(t)$ is the position of the electrons in the vacuum channel at time t . To find the maximum accelerating gradient, we need to maximize the electric field distributed in the structure, which should not exceed the material damage field. So an accelerating factor [28] ($AF = G_0/E_m$) is defined by the ratio of the accelerating gradient G_0 to the maximum electric field E_m in the structure.

A detailed geometry optimization is carried out to maximize the accelerating factor AF with the widest channel gap C . For an initial pillar height $H = 0.50\lambda_0$, a maximum accelerating factor $AF = 0.18$ can be achieved when the vacuum channel gap $C = 0.20\lambda_0$ as seen in Fig. 3(a). When C increases from $0.20\lambda_0$, the accelerating factor AF gradually decreases, which can be seen in Fig. 3(a). This means that the achievable gradient gradually drops with $C > 0.20\lambda_0$, so a channel gap of $C = 0.50\lambda_p$ is chosen as an acceptable parameter due to a trade-off between the accelerating gradient and available phase space in which high accelerating gradient occurs. As shown in Fig. 3(b), a maximum accelerating factor ($AF = 0.141$) appears at a pillar height of $H = 0.80\lambda_p$ for the structure with an optimum channel gap, $C = 0.50\lambda_p$. Fixing the grating structure, $C = 0.50\lambda_p$ and $H = 0.80\lambda_p$, we then set out to find the optimal pillar width A . Fig. 3(c) shows $AF = 0.141$ can be obtained for a pillar width $A = 0.50\lambda_p$. The longitudinal shift Δ between the gratings is also investigated. It can be seen from Fig. 3(d) that the maximum $AF = 0.141$ occurs when perfectly aligned ($\Delta = 0$ m). However, the worst shift can reduce the accelerating factor by a factor of 54% to $AF = 0.065$. The damage threshold for quartz at THz frequencies is found experimentally to be ~ 13.8 GV/m [25]. So a maximum accelerating factor of $AF = 0.141$ corresponds to a maximum achievable gradient of $0.141 \times 13.8 = 1.95$ GV/m for a quartz dual-grating structure.

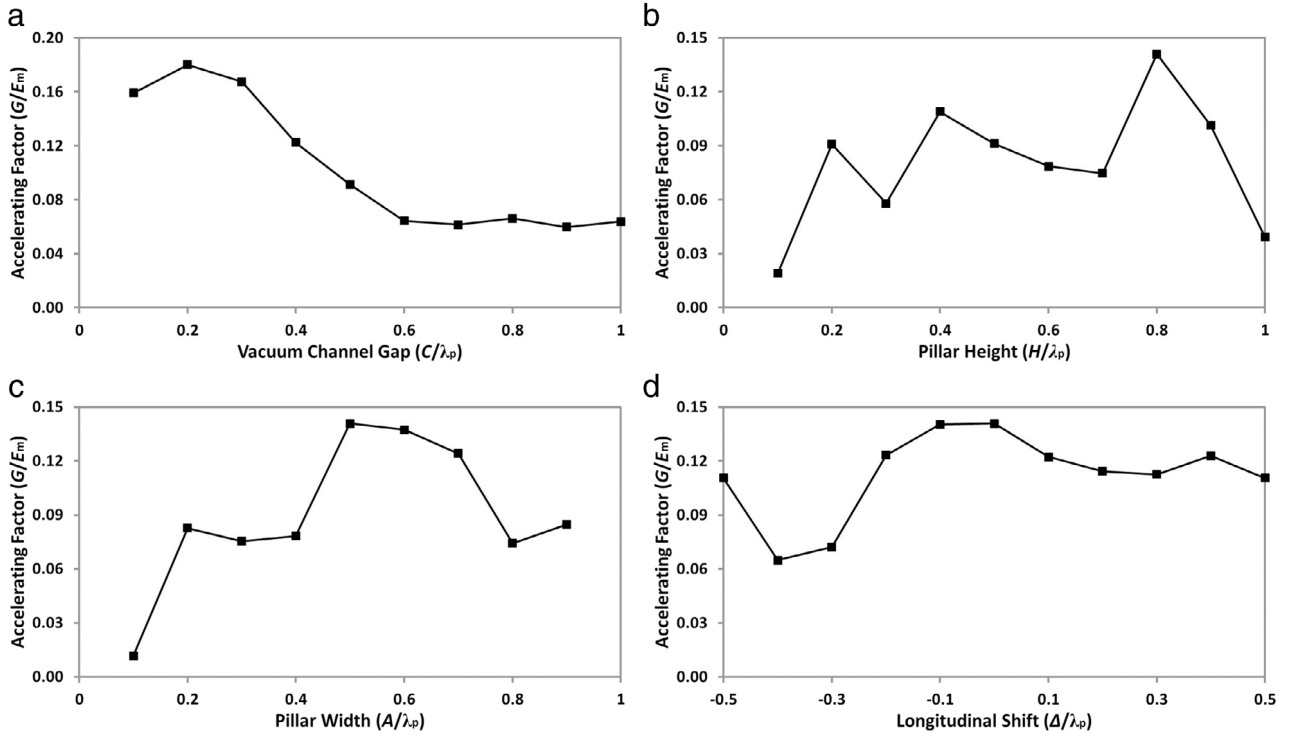


Fig. 3. FDTD optimization of accelerating factor AF as a function of (a) vacuum channel gap C with a fixed pillar height $H = 0.50\lambda_p$, (b) H with a fixed $C = 0.50\lambda_p$, (c) pillar width A with a fixed $C = 0.50\lambda_p$ and $H = 0.80\lambda_p$, and (d) longitudinal shift Δ with a fixed $C = 0.50\lambda_p$, $H = 0.80\lambda_p$ and $A = 0.50\lambda_p$.

Table 1
CLARA bunch parameters used in the simulation.

Bunch parameters	CLARA	Simulation
Bunch energy [MeV]	50	50
Bunch charge [pC]	≤ 250	0.3
Bunch RMS length [μm]	9–300	90
Bunch RMS radius [μm]	10–100	5
Normalized emittance [mm mrad]	≤ 1	0.15
Energy spread	$< 0.1\%$	0.05%

3. Wakefield study for the optimized structure

After geometry optimization, a dual-grating structure with a channel gap of $C = 0.50\lambda_p$, pillar height of $H = 0.80\lambda_p$, pillar width of $A = 0.50\lambda_p$, longitudinal shift of $\Delta = 0$ m and grating period of $\lambda_p = 150 \mu\text{m}$ is desirable as an optimum choice for the following study. In this section, detailed wakefield study are carried out by loading an electron bunch from future CLARA into such an optimized 100-period dual-grating structure without THz illumination.

The bunch parameters from future CLARA are listed in Table 1. When CLARA works at ultra-short pulse mode [21], a short electron bunch with a longitudinal RMS length of 90 μm can be generated. Assuming 10% of the initial charge of 3 pC is transmitted through the energy collimators, so an electron bunch with a charge of 0.3 pC can be obtained. Then it can be focused by a permanent magnetic quadrupole to give a transverse RMS radius of 5 μm , as shown in Table 1.

When such an electron bunch with Gaussian profiles is injected to travel along the channel center of the optimized structure without any offset in the y direction, it generates electromagnetic fields that propagate in the vacuum channel. The wakefields are reflected back by dielectric gratings and interact with the bunch itself, thus resulting in energy loss or deflection for electrons in the bunch. Here, the Wakefield Solver of CST [29] is used to calculate the wakefield generated in the optimized structure. It is then followed by a VSim Particle-In-Cell (PIC) simulation which is performed to analyze the effect of wakefield for the bunch in terms of emittance and energy spread. The longitudinal

(z -component) and transverse (y -component) wakefield distribution on z -axis in the structure are illustrated in Fig. 4. Fig. 4(a) gives a maximum longitudinal decelerating wakefield of 2.00 MV/m for the bunch. It agrees well with the final bunch energy distribution as given in Fig. 5 which gives an energy spread of 0.068% and average energy loss of $\Delta E = 30.0 \pm 1.0$ keV for the whole bunch, corresponding to a decelerating field of 2.00 ± 0.07 MV/m. In addition, the transverse wakefield, which deflects electrons, is negligible as given in Fig. 4(b) due to a small transverse size and symmetrical Gaussian profile in the y direction. This is in accordance with results from particle tracking simulations showing that when the bunch travels out of the structure, the normalized RMS emittance is still 0.15 μm , remaining the same as that of initial time.

4. THz-bunch interaction in the optimized structure

In this section, a linearly polarized Gaussian THz pulse, as shown in Fig. 6, is launched to propagate along the y -axis in order to interact with the CLARA bunch in the vacuum channel center of the optimized structure. All relevant parameters are described in Table 2. Here, the peak field of THz pulse is set to 1.0 GV/m, which can be obtained from a multi-cycle THz pulse with mJ energy proposed by K. Ravi et al. [30]. This field is still below the quartz damage threshold. In its co-moving frame, the bunch experiences the strongest field in the channel center through precise timing calculation. Considering Gaussian temporal and spatial distributions, the electrons experience a temporal electric field $E_t = G_p e^{-\left(\frac{z}{w_{\text{int}}}\right)^2}$ (Ref. [31]) with a characteristic interaction length $w_{\text{int}} = \left(\frac{1}{w_z^2} + \frac{2 \ln 2}{(\beta c \tau_p)^2}\right)^{-0.5} = 454 \mu\text{m}$. When a peak accelerating gradient of $G_p = 1.0$ GV/m is assumed for integration of this field E_t , a maximum energy gain of $\Delta E_m \approx 805$ keV is generated, which can be used to calculate the accelerating gradient for the following simulations.

A PIC simulation is then carried out using the same bunch parameters from future CLARA, so the electrons will experience a field superposition of the particle's wakefields and the driving field produced from the THz pulse. From particle tracking results, it is found that the transverse RMS

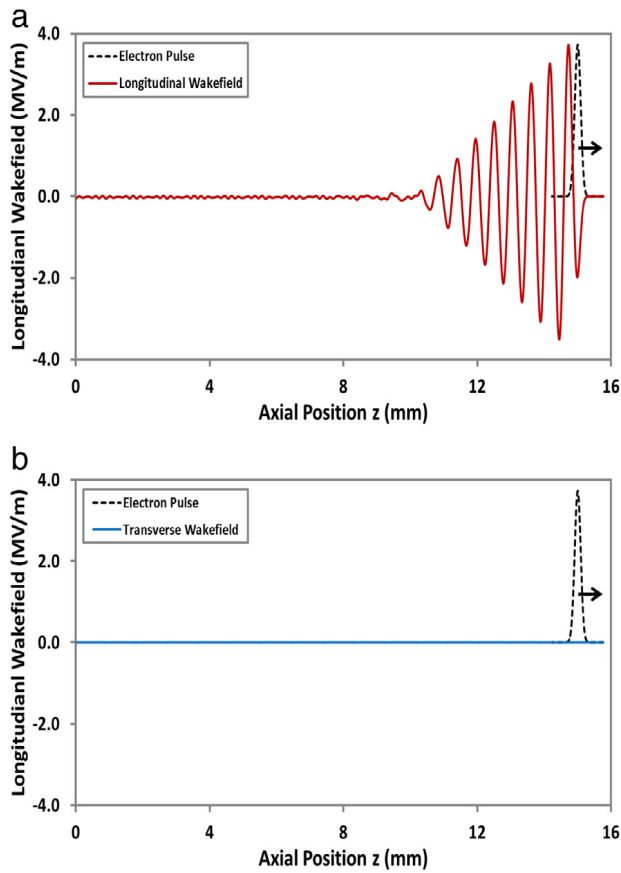


Fig. 4. Simulated longitudinal (a) and transverse (b) wakefield distribution on z -axis. The electron bunch travels along the z -axis.

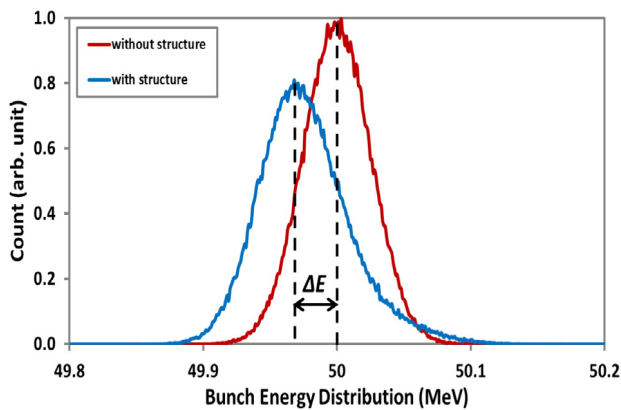


Fig. 5. The bunch energy distribution without structure (red line) shows an energy spread ~ 25 keV (0.05%) whereas the bunch going through the structure (blue line) shows an energy spread ~ 34 keV (0.068%). (For interpretation of the references to colour in this figure legend, the reader is referred to the web version of this article.)

emittance is $0.155 \mu\text{m}$ when the bunch travels out of the structure, corresponding to an increase of 3.0% compared to that of the THz-off case. This minor increment can be explained by a weak deflecting force excited by the THz pulse. However, this deflecting force does not change the bunch transverse emittance significantly at such short interaction distance. In addition, it can be compensated by a symmetric illumination using two THz pulses from opposite sides.

The electron bunch has an RMS length of $\sigma_z = 90 \mu\text{m}$, so most electrons in the range of $\pm \sigma_z$ are able to sample all phases of the THz field. Each slice of electrons ($\Delta t \ll \lambda_0/c$) samples a different phase of

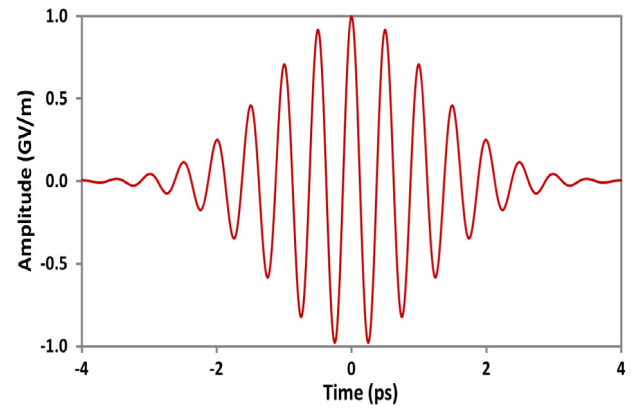


Fig. 6. The electric field envelope of the THz pulse.

Table 2

Parameters of the THz pulse used in the simulation.

THz pulse characteristics	
Propagation direction	+y
Wavelength λ	150 μm
Frequency f	2.0 THz
Peak field	1.0 GV/m
FWHM duration τ	2 ps
Waist radius w_z	1.0 mm

sinusoidal electric field in the vacuum channel and thereby experience a corresponding net energy shift $g(\Delta t, \Delta E_m) = \Delta E_m \cos\left(\frac{2\pi c}{\lambda_0} \Delta t\right)$, where ΔE_m is the maximum energy gain for the electrons. This will cause some electrons to gain energy from acceleration while others are decelerated, which generates a double-peaked profile for final bunch energy distribution, as shown in Fig. 7. The final bunch has an energy spread of 0.42% when calculated with particle tracking simulations. It is also found that the maximum energy gain is $\Delta E_m = 280 \pm 10$ keV, corresponding to a maximum accelerating gradient of $G_m = 348 \pm 12$ MV/m. Here when the peak field of a THz pulse is increased to $E_p = 3.0$ GV/m, an accelerating gradient greater than 1.0 GV/m can be expected for such a structure. It can be seen from the simulation that such a THz field of 3.0 GV/m leads to a maximum field of 9.37 GV/m, which is still below the damage threshold for quartz structures.

5. Summary and outlook

This paper presents numerical simulations for a THz-driven dual-grating structure to accelerate electrons including geometry optimizations, wakefield and THz-bunch interaction study in detail. Geometry studies have been carried out to maximize the accelerating factor with the widest channel gap C . For an optimized structure with a channel gap of $C = 0.50\lambda_p$, pillar height of $H = 0.80\lambda_p$, pillar width of $A = 0.50\lambda_p$ and longitudinal shift of $\Delta = 0$ m, a maximum accelerating factor $AF = 0.141$ can be obtained, corresponding to a maximum unloaded gradient of $G = 1.95$ GV/m. Using CST and VSim, a Gaussian electron bunch from future CLARA is loaded into an optimized 100-period structure for detailed wakefield study. When the bunch travels out of the optimized structure, the average energy is reduced by 30.0 ± 1.0 keV due to its interaction with longitudinal decelerating wakefield. The transverse wakefield can be negligible so that it does not have any effect on the bunch emittance. Then an intense THz pulse is added into simulation to interact with the CLARA bunch in the optimized structure. When the bunch propagates out of the structure, the transverse RMS emittance increases by 3.0% compared to that of THz-off case, the energy spread changes from 0.05% to 0.42%, and an accelerating gradient of 348 ± 12 MV/m could be expected from the particle tracking simulations.

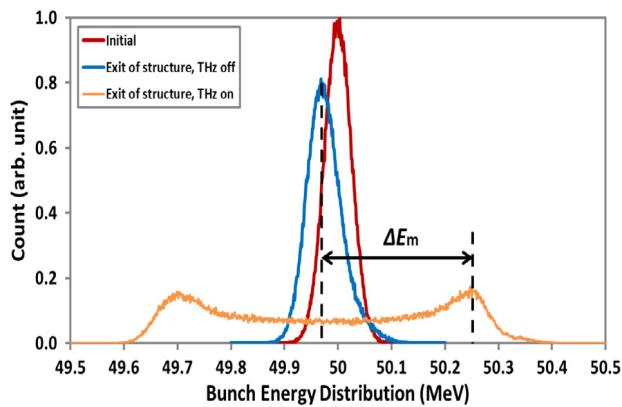


Fig. 7. The energy distribution for the initial bunch (red line), and the bunch exiting of the optimized structure when THz is off (blue line) and on (yellow line). (For interpretation of the references to colour in this figure legend, the reader is referred to the web version of this article.)

These simulations have demonstrated numerically the high gradient acceleration of electrons in a dual-grating structure driven by THz pulses, with a small emittance increase. However, there are still some technical challenges to implementing it in reality. Firstly, despite some experiments which have generated multi-cycle THz pulses with nJ [32] and μJ energies [33], further development is needed to obtain THz pulses with mJ energies, to generate the peak field of 1 GV/m which is assumed for our simulations. The second challenge is to improve the electrons' energy gain, which is limited by the short THz-bunch interaction length caused by the wide band-widths of excitation and structures. A principal option for DLAs would be to tilt the front of the laser pulses by diffraction gratings to extend the interaction length, thereby increasing the electrons' energy gain. However, THz pulses cannot be operated in a similar way due to their wide bandwidth [34]. Instead, for DTAs a multilayer dielectric Bragg reflector [12] could be incorporated into the structure to boost the accelerating field in the channel, which has the potential to increase the energy gain. Further research efforts on fabrication and experiments are still required to pave the way for a realistic high-energy DTA concept.

Acknowledgments

We would like to thank Dr. Mark Ibson for carefully proof-reading the original manuscript. This work is supported by the EU under Grant Agreement 289191 and the STFC Cockcroft Institute core grant No. ST/G008248/1.

References

- [1] W.D. Kilpatrick, Criterion for vacuum sparking designed to include both rf and dc, *Rev. Sci. Instrum.* 28 (1957) 824–826.
- [2] J.W. Wang, G.A. Loew, Field emission and rf breakdown in high-gradient room-temperature linac structures, SLAC-PUB-7684, 1997. <http://slac.stanford.edu/cgi-wrap/getdoc/slac-pub-7684.pdf>.
- [3] E.A. Peralta, K. Soong, R.J. England, E.R. Colby, Z. Wu, B. Montazeri, C. McGuinness, J. McNeur, K.J. Leedle, D. Walz, E.B. Sozer, B. Cowan, B. Schwartz, G. Travish, R.L. Byer, Demonstration of electron acceleration in a laser-driven dielectric microstructure, *Nature* 503 (2013) 91–94.
- [4] K.P. Wootton, Z. Wu, B.M. Cowan, A. Hanuka, I.V. Makasyuk, E.A. Peralta, K. Soong, R.L. Byer, R.J. England, Demonstration of acceleration of relativistic electrons at a dielectric microstructure using femtosecond laser pulses, *Opt. Lett.* 41 (2016) 2696–2699.
- [5] J. Breuer, P. Hommelhoff, Laser-based acceleration of nonrelativistic electrons at a dielectric structure, *Phys. Rev. Lett.* 111 (2013) 134803.
- [6] K.J. Leedle, R.F. Pease, R.L. Byer, J.S. Harris, Laser acceleration and deflection of 96.3 keV electrons with a silicon dielectric structure, *Optica* 2 (2015) 158–161.
- [7] K.J. Leedle, A. Ceballos, H. Deng, O. Solgaard, R.F. Pease, R.L. Byer, J.S. Harris, Dielectric laser acceleration of sub-100 keV electrons with silicon dual-pillar grating structures, *Opt. Lett.* 40 (2015) 4344–4347.
- [8] T. Plettner, P.P. Lu, R.L. Byer, Proposed few-optical cycle laser-driven particle accelerator structure, *Phys. Rev. Spec. Top. Accelerators Beams* 9 (2006) 111301.

- [9] A. Aimidula, M.A. Bake, F. Wan, B.S. Xie, C.P. Welsch, G. Xia, O. Mete, M. Uesaka, Y. Matsumura, M. Yoshida, K. Koyama, Numerically optimized structures for dielectric asymmetric dual-grating laser accelerators, *Phys. Plasmas* 21 (2014) 023110.
- [10] A. Aimidula, C.P. Welsch, G. Xia, K. Koyama, M. Uesaka, M. Yoshida, O. Mete, Y. Matsumura, Numerical investigations into a fiber laser based dielectric reverse dual-grating accelerator, *Nucl. Instrum. Methods Phys. Res. A* 740 (2014) 108–113.
- [11] Y. Wei, S. Jamison, G. Xia, K. Hanahoe, Y. Li, J.D.A. Smith, C.P. Welsch, Beam quality study for a grating-based dielectric laser-driven accelerator, *Phys. Plasmas* 24 (2017) 023102.
- [12] Y. Wei, G. Xia, J.D.A. Smith, C.P. Welsch, Dual-gratings with a bragg reflector for dielectric laser-driven accelerators, *Phys. Plasmas* 24 (2017) 073115.
- [13] J. Hebling, J.A. Fülöp, M.I. Mechler, L. Pálfalvi, C. Töke, G. Almási, preprint at <http://arxiv.org/abs/1109.6852>, 2011.
- [14] T.R. Schibli, J. Kim, O. Kuzucu, J.T. Gopinath, S.N. Tandon, G.S. Petrich, L.A. Kolodziejski, J.G. Fujimoto, E.P. Ippen, F.X. Kaertner, Attosecond active synchronization of passively mode-locked lasers by balanced cross correlation, *Opt. Lett.* 28 (2003) 947–949.
- [15] C. Vicario, A.V. Ovchinnikov, S.I. Ashtikov, M.B. Agranat, V.E. Fortov, C.P. Hauri, Generation of 0.9-mJ THz pulses in DSTMS pumped by a Cr:Mg₂SiO₄ laser, *Opt. Lett.* 39 (2014) 6632–6635.
- [16] J.A. Fülöp, Z. Ollmann, Cs. Lombosi, C. Skrobol, S. Klingebiel, L. Pálfalvi, F. Krausz, S. Karsch, J. Hebling, Efficient generation of THz pulses with 0.4 mJ energy, *Opt. Express* 22 (2014) 20155–20163.
- [17] Z. Wu, A.S. Fisher, J. Goodfellow, M. Fuchs, D. Daranciang, M. Hogan, H. Loos, A. Lindenberg, Intense terahertz pulses from SLAC electron beams using coherent transition radiation, *Rev. Sci. Instrum.* 84 (2013) 022701.
- [18] G. Andonian, D. Stratakis, M. Babzien, S. Barber, M. Fedurin, E. Hemsing, K. Kusche, P. Muggli, B. O'Shea, X. Wei, O. Williams, V. Yakimenko, J.B. Rosenzweig, Dielectric wakefield acceleration of a relativistic electron beam in a slab-symmetric dielectric lined waveguide, *Phys. Rev. Lett.* 108 (2012) 244801.
- [19] E.A. Nanni, W.R. Huang, K. Hong, K. Ravi, A. Fallahi, G. Moriena, R.J.D. Miller, F.X. Kärtner, Terahertz-driven linear electron acceleration, *Nature Commun.* 6 (2015) 8486.
- [20] B.D. O'Shea, G. Andonian, S.K. Barber, K.L. Fitzmorris, S. Hakimi, J. Harrison, P.D. Hoang, M.J. Hogan, B. Naranjo, O.B. Williams, V. Yakimenko, J.B. Rosenzweig, Observation of acceleration and deceleration in gigaelectron-volt-per-metre gradient dielectric wakefield accelerators, *Nature Commun.* 7 (2016) 12763.
- [21] J.A. Clarke, D. Angal-Kalinin, N. Bliss, R. Buckley, S. Buckley, R. Cash, P. Corlett, L. Cowie, G. Cox, G.P. Diakun, D.J. Dunning, B.D. Fell, A. Gallagher, P. Goudket, A.R. Goulden, D.M.P. Holland, S.P. Jamison, J.K. Jones, A.S. Kalinin, W. Liggins, L. Ma, K.B. Marinov, B. Martlew, P.A. McIntosh, J.W. McKenzie, K.J. Middleman, B.L. Militsyn, A.J. Moss, B.D. Muratori, M.D. Roper, R. Santer, Y. Saveliev, E. Snedden, R.J. Smith, S.L. Smith, M. Surman, T. Thakker, N.R. Thompson, R. Valizadeh, A.E. Wheelhouse, P.H. Williams, R. Bartolini, I. Martin, R. Barlow, A. Kolano, G. Burt, S. Chattopadhyay, D. Newton, A. Wolski, R.B. Appleby, H.L. Owen, M. Serluca, G. Xia, S. Boogert, A. Lyapin, L. Campbell, B.W.J. McNeil, V.V. Paramonov, CLARA conceptual design report, *J. Instrum.* 9 (05) (2014) T05001.
- [22] VSim, available from <https://www.txcorp.com/vsim>.
- [23] T. Plettner, R.L. Byer, B. Montazeri, Electromagnetic forces in the vacuum region of laser-driven layered grating structures, *J. Modern Opt.* 58 (2011) 1518–1528.
- [24] J.O. Tocho, F. Sanjuan, Optical properties of silicon, sapphire, silica and glass in the Terahertz range, in: Latin America Optics and Photonics Conference, OSA Technical Digest (Online), Paper LT4C.1, Optical Society of America, 2012.
- [25] M.C. Thompson, H. Badakov, A.M. Cook, J.B. Rosenzweig, R. Tikhoplav, G. Travish, I. Blumenfeld, M.J. Hogan, R. Ischebeck, N. Kirby, R. Siemann, D. Walz, P. Muggli, A. Scott, R.B. Yoder, Breakdown limits on gigavolt-per-meter electron-beam-driven wakefields in dielectric structures, *Phys. Rev. Lett.* 100 (2008) 214801.
- [26] A.M. Cook, R. Tikhoplav, S.Y. Tochitsky, G. Travish, O.B. Williams, J.B. Rosenzweig, Observation of narrow-band terahertz coherent Cherenkov radiation from a cylindrical dielectric-lined waveguide, *Phys. Rev. Lett.* 103 (2009) 095003.
- [27] G. Andonian, O. Williams, S. Barber, D. Bruhwiler, P. Favier, M. Fedurin, K. Fitzmorris, A. Fukasawa, P. Hoang, K. Kusche, B. Naranjo, B. O'Shea, P. Stoltz, C. Swinson, A. Valloni, J.B. Rosenzweig, Planar-dielectric-wakefield accelerator structure using Bragg-reflector boundaries, *Phys. Rev. Lett.* 113 (2014) 264801.
- [28] C.M. Chang, O. Solgaard, Silicon buried gratings for dielectric laser electron accelerators, *Appl. Phys. Lett.* 104 (2014) 184102.
- [29] CST software, available from <https://www.cst.com/>.
- [30] K. Ravi, D.N. Schimpf, F.X. Kärtner, Pulse sequences for efficient multi-cycle terahertz generation in periodically poled lithium niobate, *Opt. Express* 24 (2016) 25582–25607.
- [31] J. Breuer, R. Graf, A. Apolonski, Dielectric laser acceleration of nonrelativistic electrons at a single fused silica grating structure: experimental part, *Phys. Rev. Spec. Top. Accelerators Beams* 17 (2014) 021301.
- [32] J. Lu, H. Hwang, X. Li, S.-H. Lee, O. Pil-Kwon, K.A. Nelson, Tunable multi-cycle THz generation in organic crystal HMQ-TMS, *Opt. Express* 23 (2015) 22723–22729.
- [33] Y. Shen, X. Yang, G.L. Carr, R. Heese, Y. Hidaka, J.B. Murphy, X. Wang, Generation of tunable narrowband terahertz pulses from coherent transition radiation, Paper in Conference on Lasers and Electro-Optics, CLEO, San Jose, CA, USA, 2012.
- [34] G. Pretzler, A. Kasper, K.J. Witte, Angular chirp and tilted light pulses in CPA lasers, *Appl. Phys. B* 70 (2000) 1–9.